Fine Structure

5 One-electron atoms: fine structure and hyperfine structure

Our discussion of the energy levels and wave functions of one-electron atoms in Chapter 3 was based on the simple, non-relativistic Hamiltonian

$$H = \frac{p^2}{2\mu} - \frac{Ze^2}{(4\pi\varepsilon_0)r} \tag{5.1}$$

where the first term represents the (non-relativistic) kinetic energy of the atom in the centre of mass system, and the second term is the electrostatic (Coulomb) interaction between the electron and the nucleus. Although the energy levels obtained in Chapter 3 from the Hamiltonian (5.1) are in good agreement with experiment, the very precise measurements carried out in atomic physics demonstrate the existence of several effects which cannot be derived from the Hamiltonian (5.1) and require the addition of correction terms to (5.1). In this chapter we shall discuss these corrections.

We begin by analysing the relativistic corrections to (5.1), which give rise to a splitting of the energy levels known as fine structure. We then describe a subtle effect called the Lamb shift, which displaces the fine structure components and is therefore responsible for additional splittings of the energy levels. Finally, we consider various small corrections such as the hyperfine structure splitting and the volume effect, which take into account the fact that the nucleus is not simply a point charge, but has a finite size, and may possess an intrinsic angular momentum (spin), a magnetic dipole moment, an electric quadrupole moment, and higher moments.

5.1 Fine structure of hydrogenic atoms

The fine structure of the energy levels of hydrogenic atoms is due to relativistic effects. In order to analyse these effects we therefore need for the electron a basic wave equation which satisfies the requirements of special relativity as well as those of quantum mechanics. This is the Dirac equation, which is discussed briefly in Appendix 7, and which provides the correct relativistic wave equation for electrons.

The most rigorous way of obtaining the relativistic corrections to the Schrödinger (Bohr) energy levels of one-electron atoms is to solve the Dirac

equation for an electron in the central field $V(r) = -Ze^2/(4\pi\varepsilon_0 r)$ of the nucleus which is assumed to be of infinite mass and at the origin of the coordinates. It turns out that the Dirac equation for a central field can be separated in spherical polar coordinates and that the resulting radial equations can be solved exactly for the Coulomb potential $V(r) = -Ze^2/(4\pi\varepsilon_0 r)$ [1]. However, these calculations are rather lengthy and since the relativistic corrections are very small (provided that Z is not too large), it is convenient to use perturbation theory, keeping terms up to order v^2/c^2 in the Dirac Hamiltonian. We shall therefore start from the Hamiltonian (A7.65) of Appendix 7 which we rewrite as

$$H = H_0 + H' \tag{5.2}$$

where

$$H_0 = \frac{p^2}{2m} - \frac{Ze^2}{(4\pi\varepsilon_0)r} \tag{5.3}$$

is simply the Hamiltonian (5.1) with $\mu = m$ [2] and

$$H' = H'_1 + H'_2 + H'_3 \tag{5.4}$$

with

$$H'_1 = -\frac{p^4}{8m^3c^2} \tag{5.5}$$

$$H'_2 = \frac{1}{2m^2c^2}\frac{1}{r}\frac{\mathrm{d}V}{\mathrm{d}r}\mathbf{L}\cdot\mathbf{S} \tag{5.6}$$

and

$$H'_3 = \frac{\pi\hbar^2}{2m^2c^2}\left(\frac{Ze^2}{4\pi\varepsilon_0}\right)\delta(\mathbf{r}) \tag{5.7}$$

The physical interpretation of the three terms which constitute H' is discussed in Appendix 7. We simply note here that H'_1 is a relativistic correction to the kinetic energy, H'_2 represents the spin–orbit interaction and H'_3 is the Darwin term.

Before we proceed to the evaluation of the energy shifts due to these three terms by using perturbation theory, we remark that the Schrödinger theory discussed in Chapter 3 does not include the spin of the electron. In order to calculate

[1] See Bransden and Joachain (2000).

[2] For the sake of simplicity we shall ignore all reduced mass effects in discussing the fine structure calculations. It is of course straightforward to incorporate the reduced mass effect in H_0 and in the corresponding unperturbed energy levels E_n by replacing the electron mass m by its reduced mass μ. On the other hand, the reduced mass effects arising in H' cannot be obtained by just replacing m by μ in the results of the perturbation calculation. Fortunately, these latter reduced mass effects are very small since H' is already a correction to H_0.

corrections involving the spin operator – such as those arising from H_2' – we start from the 'unperturbed' equation

$$H_0\psi_{nlm_lm_s} = E_n\psi_{nlm_lm_s} \tag{5.8}$$

where E_n are the Schrödinger eigenvalues (3.29) (with $\mu = m$) and the zero-order wave functions $\psi_{nlm_lm_s}$ are modified (two-component) Schrödinger wave functions (also referred to as Pauli wave functions or 'spin-orbitals') given by

$$\psi_{nlm_lm_s}(q) = \psi_{nlm_l}(\mathbf{r})\chi_{1/2,m_s} \tag{5.9}$$

where q denotes the space and spin variables collectively. The quantum number m_l which can take the values $-l, -l+1, \ldots, +l$ is the magnetic quantum number previously denoted by m [3], $\psi_{nlm_l}(\mathbf{r})$ is a one-electron Schrödinger wave function (see (3.53)) such that

$$H_0\psi_{nlm_l}(\mathbf{r}) = E_n\psi_{nlm_l}(\mathbf{r}) \tag{5.10}$$

and $\chi_{1/2,m_s}$ are the spin eigenfunctions for spin one-half ($s = 1/2$) introduced in Section 2.5, with $m_s = \pm 1/2$. We recall that $\chi_{1/2,m_s}$ is a two-component spinor and that the normalised spinors corresponding respectively to 'spin up' ($m_s = +1/2$) and 'spin down' ($m_s = -1/2$) are conveniently denoted by

$$\alpha = \begin{pmatrix} 1 \\ 0 \end{pmatrix} \quad \text{and} \quad \beta = \begin{pmatrix} 0 \\ 1 \end{pmatrix} \tag{5.11}$$

Since H_0 does not act on the spin variable, the two-component wave functions (5.9) are separable in space and spin variables. It is also worth noting that we now have *four* quantum numbers (n, l, m_l, m_s) to describe a one-electron atom, the effect of the spin on the 'unperturbed' solutions being to double the degeneracy, so that each Schrödinger energy level E_n is now $2n^2$ degenerate.

Energy shifts

We now calculate the energy corrections due to the three terms (5.5)–(5.7), using the Pauli wave functions (5.9) as our zero-order wave functions.

1. $H_1' = -\dfrac{p^4}{8m^3c^2}$ (relativistic correction to the kinetic energy)

Since the unperturbed energy level E_n is $2n^2$ degenerate, we should use the degenerate perturbation theory discussed in Section 2.8. However, we first note that H_1' does not act on the spin variable. Moreover, it commutes with the components of the orbital angular momentum (see Problem 2.13) so that the perturbation

[3] When no confusion is possible, we shall continue to write m instead of m_l for the magnetic quantum number associated with the operator L_z.

H_1' is already 'diagonal' in l, m_l and m_s. The energy correction ΔE_1 due to H_1' is therefore given in first-order perturbation theory by

$$\Delta E_1 = \left\langle \psi_{nlm_l m_s} \left| -\frac{p^4}{8m^3c^2} \right| \psi_{nlm_l m_s} \right\rangle$$

$$= \left\langle \psi_{nlm_l} \left| -\frac{p^4}{8m^3c^2} \right| \psi_{nlm_l} \right\rangle$$

$$= -\frac{1}{2mc^2} \langle \psi_{nlm_l} | T^2 | \psi_{nlm_l} \rangle \tag{5.12}$$

where $T = p^2/(2m)$ is the kinetic energy operator. From (5.3) we have

$$T = H_0 + \frac{Ze^2}{(4\pi\varepsilon_0)r} \tag{5.13}$$

and therefore

$$\Delta E_1 = -\frac{1}{2mc^2} \left\langle \psi_{nlm_l} \left| \left(H_0 + \frac{Ze^2}{(4\pi\varepsilon_0)r} \right) \left(H_0 + \frac{Ze^2}{(4\pi\varepsilon_0)r} \right) \right| \psi_{nlm_l} \right\rangle$$

$$= -\frac{1}{2mc^2} \left[E_n^2 + 2E_n \left(\frac{Ze^2}{4\pi\varepsilon_0} \right) \left\langle \frac{1}{r} \right\rangle_{nlm_l} + \left(\frac{Ze^2}{4\pi\varepsilon_0} \right)^2 \left\langle \frac{1}{r^2} \right\rangle_{nlm_l} \right] \tag{5.14}$$

where we have used (5.10). From the results (3.30), (3.76) and (3.77) (with $\mu = m$) one obtains (Problem 5.1)

$$\Delta E_1 = \frac{1}{2}mc^2 \frac{(Z\alpha)^2}{n^2} \frac{(Z\alpha)^2}{n^2} \left[\frac{3}{4} - \frac{n}{l + 1/2} \right]$$

$$= -E_n \frac{(Z\alpha)^2}{n^2} \left[\frac{3}{4} - \frac{n}{l + 1/2} \right] \tag{5.15}$$

2. $H_2' = \dfrac{1}{2m^2c^2} \dfrac{1}{r} \dfrac{dV}{dr} L \cdot S$ **(spin–orbit term)**

We shall first rewrite this term more simply as

$$H_2' = \xi(r) \mathbf{L} \cdot \mathbf{S} \tag{5.16}$$

where we have introduced the quantity

$$\xi(r) = \frac{1}{2m^2c^2} \frac{1}{r} \frac{dV}{dr} \tag{5.17}$$

In our case $V(r) = -Ze^2/(4\pi\varepsilon_0 r)$, so that

$$\xi(r) = \frac{1}{2m^2c^2}\frac{Ze^2}{4\pi\varepsilon_0}\frac{1}{r^3} \tag{5.18}$$

Since the operator $\mathbf{L}^2$ does not act on the radial variable r nor on the spin variable, and commutes with the components of $\mathbf{L}$, we see from (5.16) that $\mathbf{L}^2$ commutes with H_2'. It follows that the perturbation H_2' does not connect states with different values of the orbital angular momentum l. For a given value of n and l there are $2(2l + 1)$ degenerate eigenstates of H_0 (the factor of 2 arising from the two spin states), so that the calculation of the energy shift due to H_2' requires the diagonalisation of $2(2l + 1) \times 2(2l + 1)$ submatrices.

This diagonalisation is greatly simplified by using for the zero-order wave functions a representation in which $\mathbf{L}\cdot\mathbf{S}$ is diagonal. It is clear that the functions $\psi_{nlm_lm_s}$ given by (5.9), which are simultaneous eigenfunctions of the operators H_0, $\mathbf{L}^2$, $\mathbf{S}^2$, L_z and S_z, are not adequate because $\mathbf{L}\cdot\mathbf{S}$ does not commute with L_z or S_z. However, we shall now show that satisfactory zero-order wave functions may be obtained by forming certain linear combinations of the functions $\psi_{nlm_lm_s}$. To this end, we introduce the total angular momentum of the electron

$$\mathbf{J} = \mathbf{L} + \mathbf{S} \tag{5.19}$$

and we note that

$$\mathbf{J}^2 = \mathbf{L}^2 + 2\mathbf{L}\cdot\mathbf{S} + \mathbf{S}^2 \tag{5.20}$$

so that

$$\mathbf{L}\cdot\mathbf{S} = \tfrac{1}{2}(\mathbf{J}^2 - \mathbf{L}^2 - \mathbf{S}^2) \tag{5.21}$$

Consider now wave functions ψ_{nljm_j} which are eigenstates of the operators H_0, $\mathbf{L}^2$, $\mathbf{S}^2$, $\mathbf{J}^2$ and J_z, the corresponding eigenvalues being E_n, $l(l + 1)\hbar^2$, $s(s + 1)\hbar^2$, $j(j + 1)\hbar^2$ and $m_j\hbar$. In this particular case we have $s = 1/2$ and therefore (see Section 2.5)

$$\begin{aligned} j &= l \pm 1/2, \qquad l \neq 0 \\ j &= 1/2, \qquad\quad l = 0 \end{aligned} \tag{5.22}$$

and

$$m_j = -j, -j + 1, \ldots, +j \tag{5.23}$$

By using the methods of Section 2.5 and Appendix 4, we can form the functions ψ_{nljm_j} from linear combinations of the functions $\psi_{nlm_lm_s}$ [4]. Since $\mathbf{L}\cdot\mathbf{S}$ commutes

[4] Specifically, if we use the Dirac notation so that the ket $|nlsm_lm_s\rangle$ corresponds to the wave function $\psi_{nlm_lm_s}$ and the ket $|nlsjm_j\rangle$ to the wave function ψ_{nljm_j} (with $s = 1/2$), we have

$$|nlsjm_j\rangle = \sum_{m_lm_s} \langle lsm_lm_s|jm_j\rangle\, |nlsm_lm_s\rangle$$

The Clebsch–Gordan coefficients $\langle lsm_lm_s|jm_j\rangle$ are not needed in the present calculation since we are only interested in expectation values.

with $\mathbf{L}^2$, $\mathbf{S}^2$, $\mathbf{J}^2$ and J_z it is apparent that the new zero-order wave functions ψ_{nljm_j} form a satisfactory basis set in which the operator $\mathbf{L}\cdot\mathbf{S}$ (and hence the perturbation H_2') is diagonal. Using (5.16) and (5.21), we see that for $l \neq 0$ the energy shift due to the term H_2' is given by

$$\Delta E_2 = \left\langle \psi_{nljm_j} \left| \frac{1}{2}\xi(r)[\mathbf{J}^2 - \mathbf{L}^2 - \mathbf{S}^2] \right| \psi_{nljm_j} \right\rangle$$

$$= \frac{\hbar^2}{2}\langle \xi(r) \rangle \left[j(j+1) - l(l+1) - \frac{3}{4} \right] \tag{5.24}$$

where $\langle \xi(r) \rangle$ denotes the average value of $\xi(r)$ in the state ψ_{nljm_j}. From (5.17) and (3.78), we have

$$\langle \xi(r) \rangle = \frac{1}{2m^2c^2}\left(\frac{Ze^2}{4\pi\varepsilon_0}\right)\left\langle \frac{1}{r^3} \right\rangle = \frac{1}{2m^2c^2}\left(\frac{Ze^2}{4\pi\varepsilon_0}\right)\frac{Z^3}{a_0^3 n^3 l(l+1/2)(l+1)} \tag{5.25}$$

Thus, for $l \neq 0$, one obtains from (5.24) and (5.25) (Problem 5.2)

$$\Delta E_2 = \frac{mc^2(Z\alpha)^4}{4n^3 l(l+1/2)(l+1)} \times \begin{cases} l & \text{for } j = l + 1/2 \\ -l - 1 & \text{for } j = l - 1/2 \end{cases}$$

$$= -E_n \frac{(Z\alpha)^2}{2nl(l+1/2)(l+1)} \times \begin{cases} l & \text{for } j = l + 1/2 \\ -l - 1 & \text{for } j = l - 1/2 \end{cases} \tag{5.26}$$

For $l = 0$ the spin–orbit interaction (5.16) vanishes and therefore $\Delta E_2 = 0$ in that case.

3. $H_3' = \dfrac{\pi\hbar^2}{2m^2c^2}\left(\dfrac{Ze^2}{4\pi\varepsilon_0}\right)\delta(\mathbf{r})$ (Darwin term)

This term does not act on the spin variable, is diagonal in l, m_l and m_s and applies only to the case $l = 0$. Calling ΔE_3 the corresponding energy correction and using the result (3.65), we have

$$\Delta E_3 = \frac{\pi\hbar^2}{2m^2c^2}\frac{Ze^2}{4\pi\varepsilon_0}\langle \psi_{n00} | \delta(\mathbf{r}) | \psi_{n00} \rangle$$

$$= \frac{\pi\hbar^2}{2m^2c^2}\frac{Ze^2}{4\pi\varepsilon_0}|\psi_{n00}(0)|^2$$

$$= \frac{1}{2}mc^2\frac{(Z\alpha)^2}{n^2}\frac{(Z\alpha)^2}{n}$$

$$= -E_n\frac{(Z\alpha)^2}{n}, \qquad l = 0 \tag{5.27}$$

We may now combine the effects of H_1', H_2' and H_3' to obtain the total energy shift $\Delta E = \Delta E_1 + \Delta E_2 + \Delta E_3$ due to relativistic corrections. From (5.15), (5.26) and (5.27) we have for all l (Problem 5.3)

$$\Delta E_{nj} = -\frac{1}{2}mc^2\frac{(Z\alpha)^2}{n^2}\frac{(Z\alpha)^2}{n^2}\left(\frac{n}{j+1/2} - \frac{3}{4}\right)$$

$$= E_n\frac{(Z\alpha)^2}{n^2}\left(\frac{n}{j+1/2} - \frac{3}{4}\right) \tag{5.28}$$

where the subscripts nj indicate that the correction depends on both the principal quantum number n and the total angular momentum quantum number j, with $j = 1/2, 3/2, \ldots, n - 1/2$. To each value of j correspond two possible values of l given by $l = j \pm 1/2$, except for $j = n - 1/2$ where one can only have $l = j - 1/2 = n - 1$.

Adding the relativistic correction ΔE_{nj} to the non-relativistic energy E_n, we find that the energy levels of one-electron atoms are now given by

$$E_{nj} = E_n\left[1 + \frac{(Z\alpha)^2}{n^2}\left(\frac{n}{j+1/2} - \frac{3}{4}\right)\right] \tag{5.29}$$

so that the binding energy $|E_{nj}|$ of the electron is slightly increased with respect to the non-relativistic value $|E_n|$, the absolute value $|\Delta E_{nj}|$ of the energy shift becoming smaller as n or j increases, and larger as Z increases. The formula (5.29) can be shown (Problem 5.4) to agree up to order $(Z\alpha)^2$ with the result

$$E_{nj}^{\text{exact}} = mc^2\left\{\left[1 + \left(\frac{Z\alpha}{n - j - 1/2 + [(j+1/2)^2 - Z^2\alpha^2]^{1/2}}\right)^2\right]^{-1/2} - 1\right\} \tag{5.30}$$

obtained by solving the Dirac equation for the potential $V(r) = -Ze^2/(4\pi\varepsilon_0 r)$ [1].

Fine structure splitting

Starting from non-relativistic energy levels E_n which are $2n^2$ times degenerate (the factor of two arising from the spin) we see that in the Dirac theory this degeneracy is partly removed. In fact, a non-relativistic energy level E_n depending only on the principal quantum number n splits into n different levels in the Dirac theory, one for each value $j = 1/2, 3/2, \ldots, n - 1/2$ of the total angular momentum quantum number j. This splitting is called *fine structure splitting*, and the n levels $j = 1/2, 3/2, \ldots, n - 1/2$ are said to form a *fine structure multiplet*. We note that the dimensionless constant $\alpha \simeq 1/137$ controls the scale of the splitting, and it is for this reason that it has been called the fine structure constant.

The fine structure splitting of the energy levels corresponding to $n = 1, 2, 3$ is illustrated in Fig. 5.1. We have used in that figure the spectroscopic notation nl_j (with the usual association of the letters s, p, d, ... with the values $l = 0, 1, 2, \ldots$

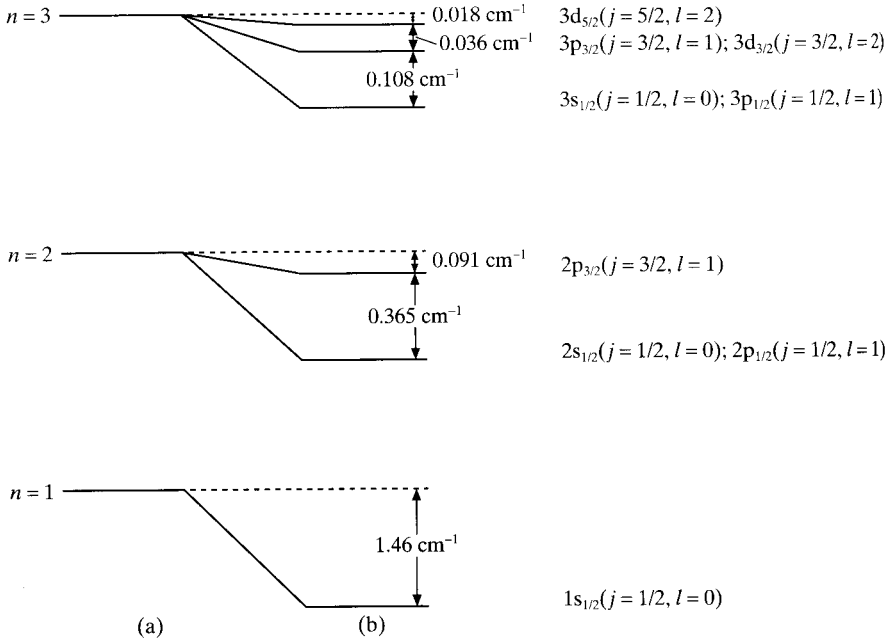

Figure 5.1 Fine structure of the hydrogen atom. The non-relativistic levels are shown on the left in column (a) and the split levels on the right in column (b), for $n = 1$, 2 and 3. For clarity, the scale in each diagram is different.

and an additional subscript for the value of j) to distinguish the various spectral terms corresponding to the Dirac theory [5].

It is important to emphasise that in Dirac's theory two states having the same value of the quantum number n and j but with values of l such that $l = j \pm 1/2$ have the same energy. The *parity* of the solutions is still given by $(-)^l$. Thus to each value of j correspond two series of $(2j + 1)$ solutions of opposite parity, except for $j = n - 1/2$ where there is only one series of solutions of parity $(-)^{n-1}$. It is also worth remarking that although the three separate contributions ΔE_1, ΔE_2 and ΔE_3 depend on l (see (5.15), (5.26) and (5.27)), the total energy shift ΔE_{nj} (given by (5.28)) does not! This is illustrated in Fig. 5.2, where we show the splitting of the $n = 2$ levels of atomic hydrogen due to each of the three terms H_1', H_2' and H_3', as well as the resulting degeneracy of the $2s_{1/2}$ and $2p_{1/2}$ levels. We shall see in Section 5.2 that this degeneracy of the levels with $l = j \pm 1/2$ is actually removed by small quantum electrodynamics effects, known as *radiative corrections*, which are responsible for additional energy shifts called *Lamb shifts*.

[5] A similar notation with capital letters, such as $1S_{1/2}$, $2S_{1/2}$, $2P_{1/2}$, $2P_{3/2}$, etc., is also frequently used.

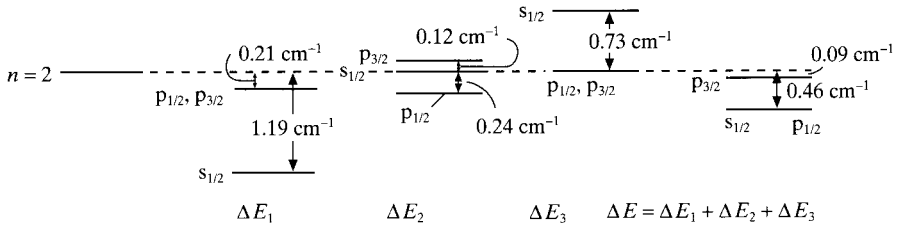

Figure 5.2 The contributions ΔE_1, ΔE_2, ΔE_3 to the splitting of the $n = 2$ level of the hydrogen atom.

Another interesting point is that the three relativistic energy shifts ΔE_1, ΔE_2 and ΔE_3 we have obtained above have the same order of magnitude, and must therefore be treated together. This is a special feature of hydrogenic atoms. For many-electron atoms (and in particular for alkali atoms) we shall see in Chapter 8 that it is the spin–orbit effect (due here to the term H_2') which is mainly responsible for the fine structure splitting.

According to (5.28), for any Z and $n \neq 1$, the energy difference between the two extreme components of a fine structure multiplet (corresponding respectively to the values $j_1 = n - 1/2$ and $j_2 = 1/2$) is given by

$$\delta E(j_1 = n - 1/2, j_2 = 1/2) = |E_n|(Z\alpha)^2 \frac{n-1}{n^2}$$

$$= \frac{\alpha^2 Z^4 (n-1)}{2n^4} \quad \text{a.u.}, \quad n \neq 1 \tag{5.31}$$

We may also use (5.28) to obtain for any Z, $n \neq 1$ and $l \neq 0$ the energy separation between two levels corresponding respectively to $j_1 = l + 1/2$ and $j_2 = l - 1/2$. The result is

$$\delta E(j_1 = l + 1/2, j_2 = l - 1/2) = |E_n| \frac{(Z\alpha)^2}{nl(l+1)}$$

$$= \frac{\alpha^2 Z^4}{2n^3 l(l+1)} \quad \text{a.u.} \tag{5.32}$$

For example, in the case of atomic hydrogen the splitting of the levels $j = 3/2$ and $j = 1/2$ for $n = 2$ and $n = 3$ is, respectively, 0.365 cm^{-1} (4.52×10^{-5} eV) and 0.108 cm^{-1} (1.34×10^{-5} eV), while the splitting of the levels $j = 5/2$ and $j = 3/2$ for $n = 3$ is 0.036 cm^{-1} (4.48×10^{-6} eV) as shown in Fig. 5.1.

Fine structure of spectral lines

The set of *spectral lines* due to the transitions $nlj \rightarrow n'l'j'$ between the fine structure components of the levels nl and $n'l'$ is known as a *multiplet* of lines. Since the

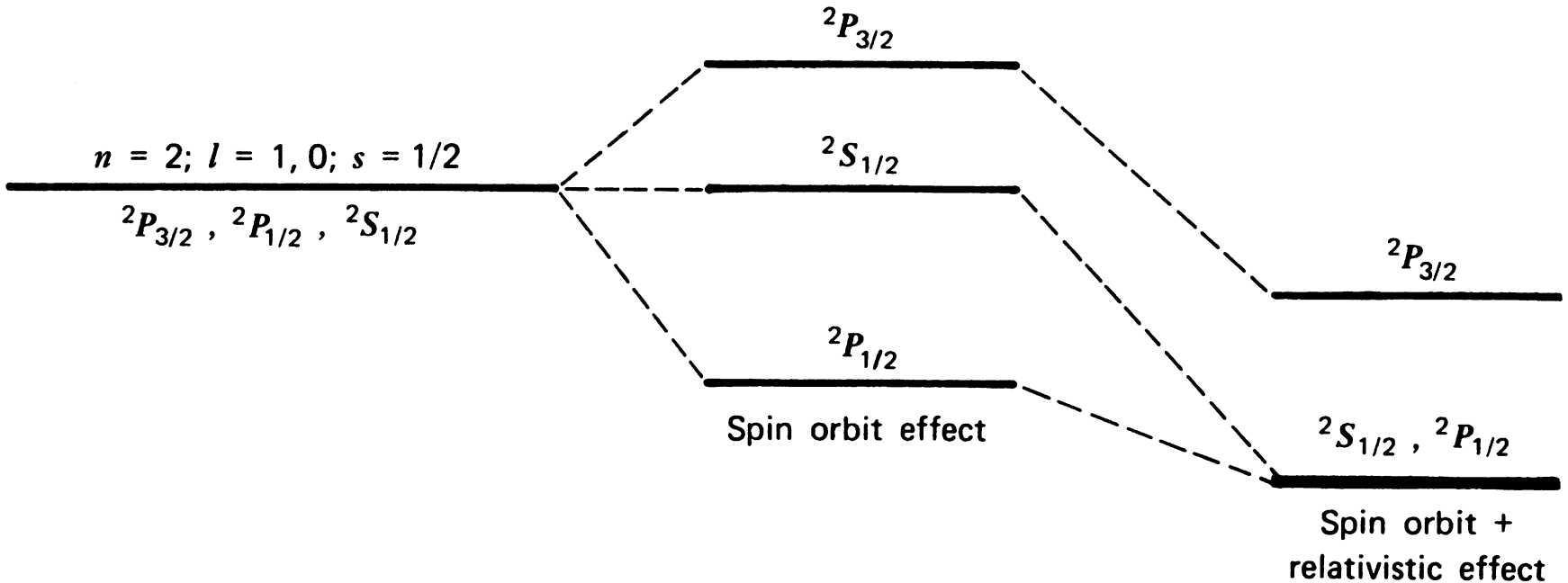

Figure 17-1. Splitting of the $n = 2$ levels by (1) the spin-orbit coupling (which leaves the S state unaffected) and (2) the relativistic effect. The final degeneracy of the $^2S_{1/2}$ and $^2P_{1/2}$ states is actually lifted by quantum electrodynamic effects. The tiny upward shift of the $^2S_{1/2}$ state is called the Lamb shift.

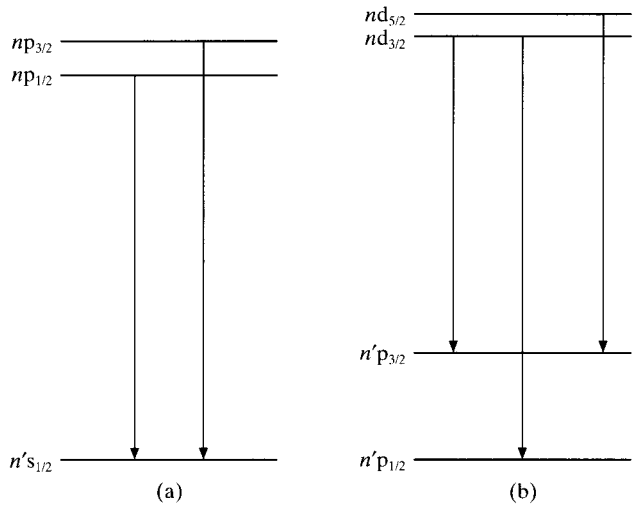

Figure 5.3 Allowed transitions in the multiplets (a) $np - n's$ and (b) $nd - n'p$.

electric dipole operator $\mathbf{D} = -e\mathbf{r}$ does not depend on the spin, the selection rule derived in Chapter 4 for the quantum number l (in the dipole approximation) remains

$$\Delta l = \pm 1 \tag{5.33}$$

from which it follows that the selection rule with respect to the quantum number j is

$$\Delta j = 0, \pm 1 \tag{5.34}$$

Using (5.33) and (5.34), it is a simple matter to establish the character of the fine structure splitting of the hydrogenic atom spectral lines. For example, we see from Fig. 5.3 that the multiplet np–$n's$ has two components. Thus each line of the Lyman series (lower state $n = 1$) is split by the fine structure into a pair of lines called a *doublet*, corresponding to the transitions

$$np_{1/2}\text{–}1s_{1/2}, \qquad np_{3/2}\text{–}1s_{1/2}$$

This is illustrated in Fig. 5.4 for the Lyman α line (upper state $n = 2$).

Referring to Fig. 5.3, we see that the multiplet np–$n's$ has two components, while the multiplet nd–$n'p$ has three components. Thus, in the case of the Balmer series (lower state $n = 2$) the following seven transitions are allowed:

$$np_{1/2}\text{–}2s_{1/2}, \qquad np_{3/2}\text{–}2s_{1/2}$$
$$ns_{1/2}\text{–}2p_{1/2}, \qquad ns_{1/2}\text{–}2p_{3/2}$$
$$nd_{3/2}\text{–}2p_{1/2}, \qquad nd_{3/2}\text{–}2p_{3/2}$$
$$nd_{5/2}\text{–}2p_{3/2}$$

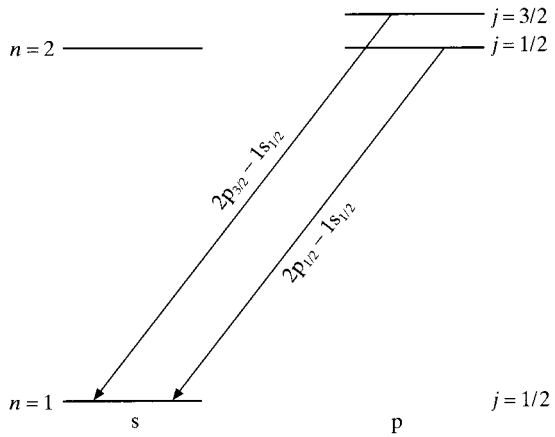

Figure 5.4 Allowed transitions between the $n = 2$ and $n = 1$ levels of atomic hydrogen giving rise to the Lyman alpha doublet (L_α).

However, since the levels $ns_{1/2}$ and $np_{1/2}$ coincide, as well as the levels $np_{3/2}$ and $nd_{3/2}$, each Balmer line only contains five distinct components. This is illustrated in Fig. 5.5 for the case of the fine structure of the H_α line, that is the red line of the Balmer series at 6563 Å, corresponding to the transition between the upper state $n = 3$ and the lower state $n = 2$.

Because the energy differences (5.31) or (5.32) rapidly decrease with increasing n, the fine structure splitting of a spectral line corresponding to a transition between two levels of different n is mainly due to the fine structure of the *lower* level, with additional (finer) fine structure arising from the smaller splitting of the upper level. For example, each line of the Balmer series essentially consists of a *doublet*, or more precisely of *two groups* of closely spaced lines. The distance between these two groups is approximately given by the fine structure splitting of the lower ($n = 2$) level (that is, about 0.365 cm^{-1}) and this distance is constant for all the lines of the series. Within each of the two groups the magnitude of the (small) residual splitting due to the fine structure of the upper level rapidly falls off as n increases, that is as one goes to higher lines of the series. Similarly, each line of the Paschen series (lower state $n = 3$) consists of *three groups* of closely spaced lines, etc. Finally, we remark that for hydrogenic ions the fine structure splitting is more important than for hydrogen since the energy shift ΔE_{nj} given by (5.28) is proportional to Z^4.

Intensities of fine structure lines

Since the radial integrals in (4.113) are the same for both the transitions $np_{3/2}$–$n's_{1/2}$ and $np_{1/2}$–$n's_{1/2}$, it is easy to obtain from the angular parts of those integrals (that

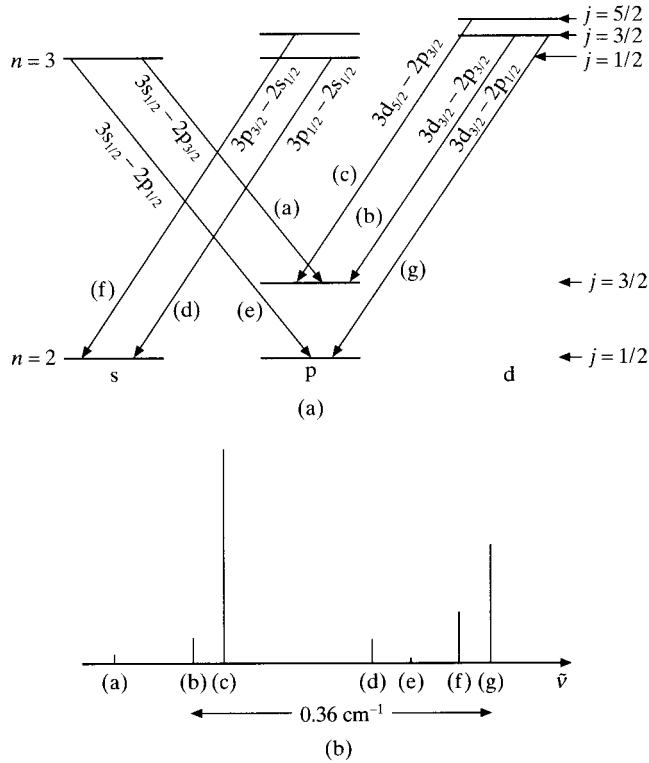

Figure 5.5 (a) Transitions contributing to the Balmer alpha (H_α) line between the $n = 3$ and $n = 2$ levels of atomic hydrogen.
(b) The observed relative intensities of the lines (a), (b)–(g). Note that (b) and (g) have the same upper level, so that the wave number difference between the lines is determined by the $2p_{1/2} - 2p_{3/2}$ energy difference and is 0.36 cm^{-1}. In the same way, the wave number difference between lines (a) and (e) is also 0.36 cm^{-1}. The lines (d) and (e) should coincide according to Dirac theory, as well as the lines (f) and (g); the differences are due to the Lamb shift.

is, from angular momentum considerations) the ratio of the two transition probabilities, which is found to be equal to 2 (Problem 5.5). More generally, the ratios of the transition probabilities for the most important special cases are (Bethe and Salpeter, 1957)

$$\begin{aligned} \text{for} \quad & \text{sp transitions: } s_{1/2}\text{–}p_{3/2}\text{:}s_{1/2}\text{–}p_{1/2} = 2\text{:}1 \\ & \text{pd transitions: } p_{3/2}\text{–}d_{5/2}\text{:}p_{3/2}\text{–}d_{3/2}\text{:}p_{1/2}\text{–}d_{3/2} = 9\text{:}1\text{:}5 \\ & \text{df transitions: } d_{5/2}\text{–}f_{7/2}\text{:}d_{5/2}\text{–}f_{5/2}\text{:}d_{3/2}\text{–}f_{5/2} = 20\text{:}1\text{:}14 \end{aligned} \tag{5.35}$$

Under most circumstances the initial states are excited in proportion to their statistical weights, that is the $(2j + 1)$ degenerate levels corresponding to an initial state with a given value of j (but differing in $m_j = -j, -j + 1, \ldots, +j$) are equally

Lamb Shift

populated. In this case the ratios of line intensities are the same as those of the corresponding transition probabilities. The relative intensities of the fine structure components of the H_α line are shown in Fig. 5.5.

Comparison with experiment

Many spectroscopic studies of the fine structure of atomic hydrogen and hydrogenic ions (in particular He^+) were made to test the Dirac theory, but no definite conclusion had been reached by 1940. Although there was some evidence strongly supporting the theory, the measurements performed by W.V. Houston in 1937 and R.C. Williams in 1938 were interpreted in 1938 by S. Pasternack as indicating that the $2s_{1/2}$ and $2p_{1/2}$ levels did not coincide exactly, but that there existed a slight upward shift of the $2s_{1/2}$ level with respect to the $2p_{1/2}$ level of about 0.03 cm^{-1}. However, the experimental attempts to obtain accurate information about the fine structure of hydrogenic atoms were frustrated by the broadening of the spectral lines, due mainly to the Doppler effect. In fact, other spectroscopists disagreed with the results of Houston and Williams, and found no discrepancy with the Dirac theory.

The question was settled in 1947 by W.E. Lamb and R.C. Retherford, who demonstrated in a decisive way the existence of an energy difference between the two levels $2s_{1/2}$ and $2p_{1/2}$. This 'Lamb shift', to which we have already alluded in the discussion following (5.30), will now be considered.

5.2 The Lamb shift

Instead of attempting to resolve the fine structure of hydrogen by investigating its optical spectrum, Lamb and Retherford used *microwave techniques* [6] to stimulate a direct *radio-frequency* transition between the $2s_{1/2}$ and $2p_{1/2}$ levels. As we noted in Section 4.5 there is no selection rule on the principal quantum number n for electric dipole transitions. In particular, these transitions can occur between levels having the *same* principal quantum number. This fact was pointed out as early as 1928 by W. Grotrian, who suggested that it should be possible with radio waves to induce such transitions among the excited states of the hydrogen atom. For example, in the case of the transition $2s_{1/2}$–$2p_{3/2}$, the energy separation $\delta E = 4.52 \times 10^{-5}$ eV = 0.365 cm^{-1} which we obtained in (5.32) corresponds to a wavelength of 2.74 cm or a frequency of 10 949 MHz. Because the frequencies of radio waves are much smaller than those corresponding to optical lines (such as the H_α line), the Doppler broadening, which is proportional to the frequency (see (4.192)), is considerably reduced in radio-frequency experiments, and could in fact be neglected in the experiment of Lamb and Retherford. Of course, since

[6] A detailed account of microwave spectroscopy may be found in Townes and Schawlow (1975).

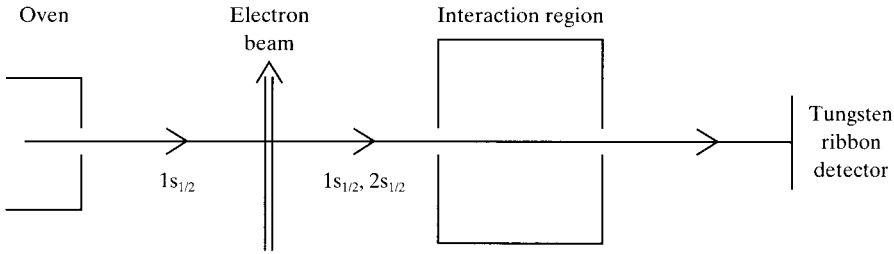

Figure 5.6 Schematic diagram of the Lamb–Retherford experiment. A collimated beam of hydrogen atoms emerges from an oven. A fraction of the atoms is excited to the $n = 2$ level by electron bombardment. The beam then passes through a region of radio-frequency electric field and a variable magnetic field, and is detected by an apparatus which records only atoms in the $n = 2$ level.

the frequencies of radio waves are small, the transition rates for spontaneous emission, which are proportional to ν^3 (see (4.80)) are very small. However, *stimulated* (induced) transitions can occur if the atoms are sent through a region where there is an electric field oscillating at the appropriate frequency corresponding to the transition to be studied. In the experiment of Lamb and Retherford such stimulated transitions are observed between the levels $2s_{1/2}$–$2p_{1/2}$ and $2s_{1/2}$–$2p_{3/2}$. Since the transition rates for stimulated absorption and emission are equal (see (4.50)), it is necessary that the two states between which the transitions are studied should be unequally populated.

The experimental method of Lamb and Retherford is based on the fact that the $2s_{1/2}$ level is *metastable*. Indeed, as we have seen in Chapter 4, the electric dipole transition from the state $2s_{1/2}$ to the ground state $1s_{1/2}$ is forbidden by the selection rule $\Delta l = \pm 1$. The most probable decay mechanism of the $2s_{1/2}$ state is two-photon emission, with a lifetime of 1/7 s. Thus, in the absence of perturbations, the lifetime of the $2s_{1/2}$ state is very long compared to that of the 2p states, which is about 1.6×10^{-9} s. In the apparatus of Lamb and Retherford, shown in Fig. 5.6, a beam of atomic hydrogen containing atoms in the metastable $2s_{1/2}$ state is produced by first dissociating molecular hydrogen in a tungsten oven (at a temperature of 2500 K where the dissociation is about 64 per cent complete), selecting a jet of atoms by means of slits, and bombarding this jet with a beam of electrons having a kinetic energy somewhat larger than 10.2 eV, which is the threshold energy for excitation of the $n = 2$ levels of atomic hydrogen. In this way a small fraction of hydrogen atoms (about one in 10^8) is excited to the $2s_{1/2}$, $2p_{1/2}$ and $2p_{3/2}$ states. The average velocity of the atomic beam is about 8×10^5 cm s^{-1}. Because of their long lifetime, the atoms in the metastable $2s_{1/2}$ state can easily reach a detector placed at a distance of about 10 cm from the region where they are produced. On the other hand the atoms which are excited in the $2p_{1/2}$ or $2p_{3/2}$ states quickly decay to the ground state $1s_{1/2}$ in 1.6×10^{-9} s, moving only about 1.3×10^{-3} cm in that time, so that they cannot reach the detector. This detector is a metallic surface (a tungsten

ribbon), from which the atoms in the metastable state $2s_{1/2}$ can eject electrons by giving up their excitation energy. Atoms in the ground state are not detected, the measured electronic current being proportional to the number of metastable atoms reaching the detector. Now, if the beam containing the metastable $2s_{1/2}$ atoms passes through an 'interaction region' in which a radio-frequency field of the proper frequency is applied, the metastable atoms will undergo induced transitions to the $2p_{1/2}$ and $2p_{3/2}$ states, and decay to the ground state $1s_{1/2}$ in which they are not detected. As a result, there is a reduction of the number of metastable ($2s_{1/2}$) atoms registered by the detector at the (resonant) radio frequencies corresponding to the frequencies of the $2s_{1/2}$–$2p_{1/2}$ and $2s_{1/2}$–$2p_{3/2}$ transitions. In the 'interaction region' the atomic beam also passes in a variable magnetic field. In this way Lamb and Retherford could not only separate the Zeeman components of the $2s_{1/2}$, $2p_{1/2}$ and $2p_{3/2}$ levels, but also reduce the probability of fortuitious depletion of the $2s_{1/2}$ state due to Stark effect mixing of the $2s_{1/2}$ and the 2p levels caused by perturbing electric fields, as we shall see in Chapter 6. Moreover, the use of a variable external magnetic field avoids the difficulty of producing a radio-frequency field with a variable frequency but a constant radio-frequency power. Instead, Lamb and Retherford could operate at a fixed frequency of the radio-frequency field and obtain the passage through the resonance by varying the magnetic field. The resonance frequency for zero magnetic field was found by extrapolation. In this way Lamb and Retherford found in 1947 that the $2s_{1/2}$ level lies above the $2p_{1/2}$ level by an amount of about 1000 MHz. Further experiments carried out in 1953 by S. Triebwasser, E.S. Dayhoff and W.E. Lamb gave the very precise value (1057.77 ± 0.10) MHz for this energy difference, which is now called a 'Lamb shift'. We note that this value, which corresponds to $4.374\,62 \times 10^{-6}$ eV or $0.035\,283\,4$ cm^{-1}, is about one-tenth of the fine structure splitting of the $n = 2$ term.

The need to explain the Lamb shift stimulated numerous theoretical developments which led H.A. Bethe, S. Tomonaga, J. Schwinger, R.P. Feynman and F.J. Dyson to fundamental revisions of physical concepts (such as the renormalisation of mass) and to the formulation of the theory of *quantum electrodynamics* (QED). In this theory, 'radiative corrections' to the Dirac theory are obtained by taking into account the interaction of the electron with the quantised electromagnetic field. These calculations are outside the scope of this book, and we only mention the following qualitative explanation of the Lamb shift given in 1948 by T.A. Welton. A quantised radiation field in its lowest energy state is not one with zero electromagnetic fields, but there exist zero-point oscillations similar to those we discussed for the case of the harmonic oscillator in Section 2.4. This means that even in the vacuum there are fluctuations in this zero-point radiation field which can act on the electron, causing it to execute rapid oscillatory motions so that its charge is 'smeared out' and the point electron effectively becomes a sphere of a certain radius. If the electron is bound by a non-uniform electric field, as in atomic systems, it will therefore experience a potential which is slightly different from that corresponding to its mean position. In particular, the electron in a

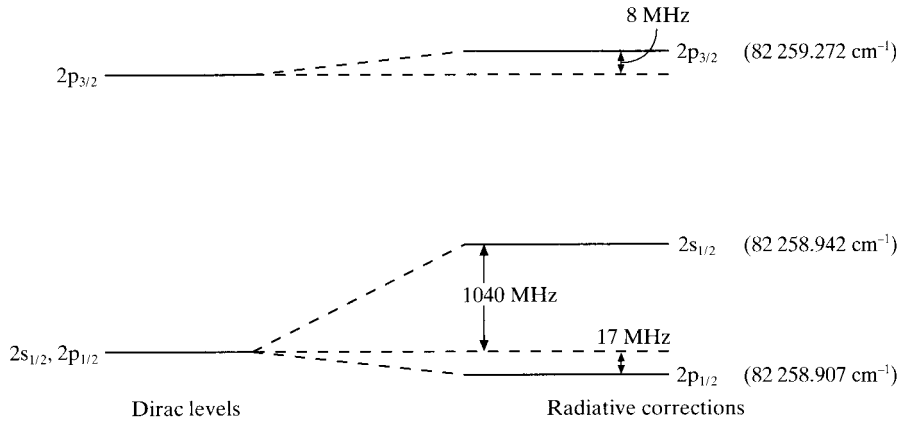

Figure 5.7 Diagram (not to scale) showing the calculated energy shifts due to radiative corrections to the Dirac theory for the $n = 2$ levels of atomic hydrogen.

one-electron atom is not so strongly attracted to the nucleus at short distances. As a result, s states (which are most sensitive to short-distance modifications because $|\psi(0)|^2 \neq 0$ for these states) are raised in energy with respect to other states, for which the corresponding modifications are much smaller.

The calculated energy shifts for the $2s_{1/2}$, $2p_{1/2}$ and $2p_{3/2}$ levels with respect to the Dirac theory are illustrated in Fig. 5.7 for the case of atomic hydrogen. The theoretical value for the Lamb shift (the energy difference between the $2s_{1/2}$ and $2p_{1/2}$ levels) calculated in 1971 by G.W. Erickson is (1057.916 ± 0.010) MHz and that obtained in 1975 by P.J. Mohr is (1057.864 ± 0.014) MHz. Both calculations are in excellent agreement with the experimental value of (1057.77 ± 0.10) MHz measured in 1953 by Lamb and his co-workers, and with more recent experiments [7]. In particular, R.T. Robiscoe and T.W. Shyn measured in 1970 the value (1057.90 ± 0.06) MHz, S.R. Lundeen and F.M. Pipkin found the result (1057.893 ± 0.020) MHz and D.A. Andrews and G. Newton found the value (1057.862 ± 0.020) MHz.

It is also possible to measure the Lamb shift by resolving the Balmer alpha (H_α) line (see Fig. 5.5) using the method of *saturation (Doppler-free) spectroscopy*, which will be described in Section 15.2. We show in Fig. 5.8 the results obtained in this way by T.W. Hänsch, I.S. Shahin and A.L. Schawlow in 1972, compared with the Doppler-broadened H_α line, as it can be observed at room temperature using conventional spectroscopy.

The Lamb shift has also been measured and calculated for other levels of atomic hydrogen and for other hydrogenic systems such as deuterium, He^+ and hydrogen-like multiply charged ions. As an example, we show in Fig. 5.9 the

[7] A detailed account of Lamb shift experiments and calculations can be found in Series (1988).

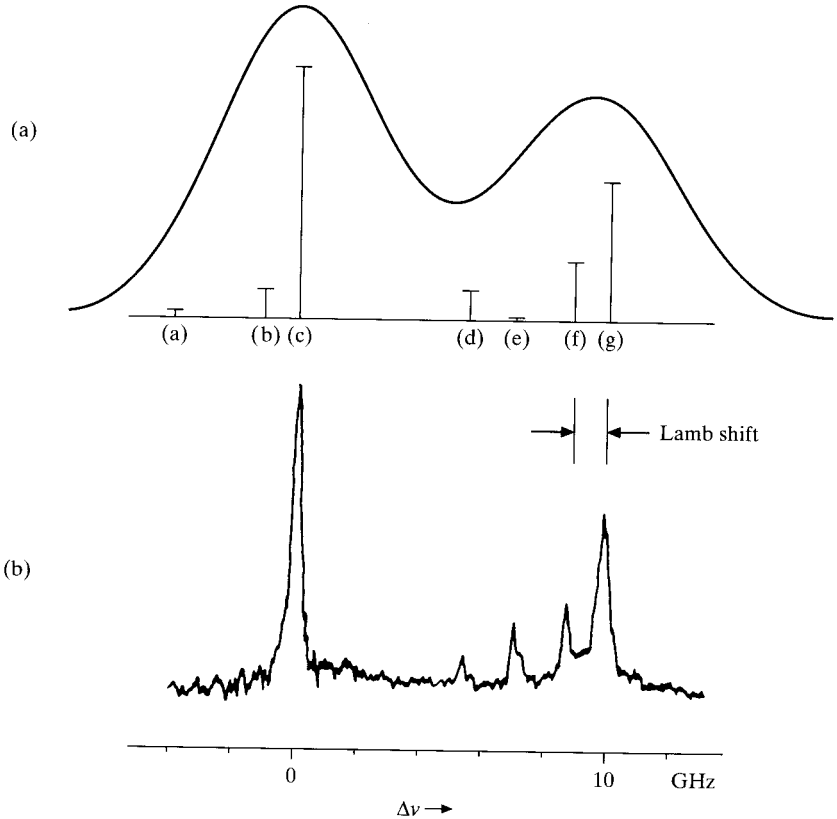

Figure 5.8 (a) The structure of the Balmer alpha (H_α) line, as observed by conventional spectroscopy with Doppler broadening at room temperature (300 K). The lines marked (a), (b)–(g) refer to those shown in Fig. 5.5.
(b) The fully resolved structure of the H_α line obtained by saturation spectroscopy (after T.W. Hänsch *et al.*).

$n = 1$ and $n = 2$ energy levels of hydrogen-like U^{91+} according to the Dirac theory, and with QED corrections. The size of these corrections increases rapidly with increasing Z. In particular, the value of the $2s_{1/2}$–$2p_{1/2}$ Lamb shift is 75 eV for U^{91+}. It is interesting to note that for one-electron ions with high Z the dominant decay mechanism of the $2s_{1/2}$ state is not two-photon emission, but single photon emission through a magnetic dipole (M1) transition. The measured values of the $2p_{3/2} \rightarrow 1s_{1/2}$ and $2s_{1/2}$, $2p_{1/2} \rightarrow 1s_{1/2}$ energy differences in U^{91+}, obtained in 1993 by Th. Stöhlker *et al.* (who performed X-ray experiments using a heavy ion storage ring), are given by 102.209 keV and 97.706 keV, respectively. The corresponding theoretical values, calculated in 1985 by W.R. Johnson and G. Soff, are 102.180 keV and 97.673 keV.

Hyperfine Structure

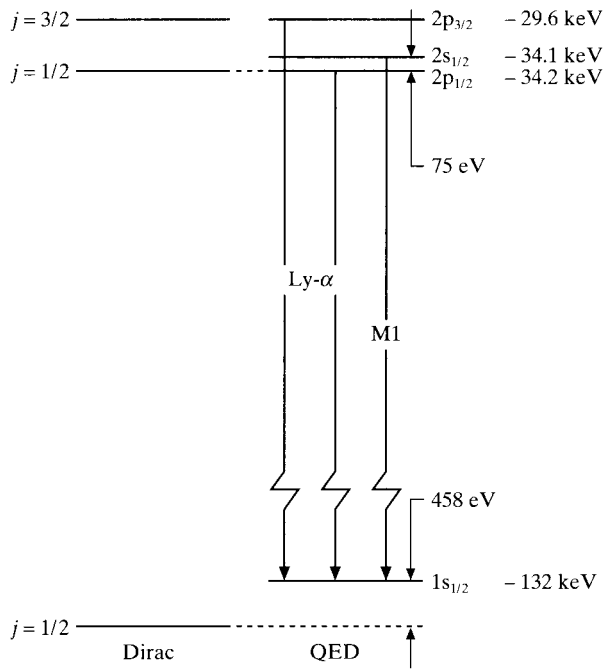

Figure 5.9 The $n = 1$ and $n = 2$ energy levels of U^{91+} according to the Dirac theory and with QED corrections.

5.3 Hyperfine structure and isotope shifts

Atomic nuclei have radii of the order of 10^{-4} Å (10^{-14} m) which are very small compared with typical distances of an electron from the nucleus (~1 Å). The nuclei are also much heavier (about 10^4 times) than electrons. It is therefore a very good approximation to consider the nuclei to be positive point charges of infinite mass. However, the high-precision experiments which can be carried out in atomic physics reveal the existence of tiny effects on the electronic energy levels, which cannot be explained if the nuclei are considered to be point charges of infinite mass. These effects, first observed by A. Michelson in 1891 and C. Fabry and A. Perot in 1897, are called *hyperfine effects*, because they produce shifts of the electronic energy levels which are usually much smaller than those corresponding to the fine structure studied in Section 5.1.

It is convenient to classify the hyperfine effects into those which give rise to *splittings* of the electronic energy levels, and those which slightly shift the energy levels, but without giving rise to splittings. The former are called *hyperfine structure* effects while the latter are known as *isotope shifts* (or isotope effects) since they can usually be detected only by examining their variation between two or more isotopes. We have already encountered examples of isotopic shifts in

Chapters 1 and 3, when we studied the modification of the energy levels of hydrogenic atoms due to the fact that *the nuclear mass is finite* (reduced mass effect). In particular, we saw that the introduction of the reduced mass gives a very good account of the frequency difference between the spectral lines of 'ordinary' atomic hydrogen (proton + electron) and its heavy isotope, deuterium (deuteron + electron). Another isotope shift is the *volume effect*, which arises because the nuclear charge is distributed within a finite volume, so that the potential felt by the electron is modified at short distances. We shall briefly consider this effect at the end of this section.

Let us now turn our attention to the *hyperfine structure effects*, which are responsible for splittings (extending over the range from 10^{-3} to 1 cm^{-1}) of the energy levels of the atoms. These effects result from the fact that a nucleus may possess *electromagnetic multipole moments* (of higher order than the electric monopole) which can interact with the electromagnetic field produced at the nucleus by the electrons. By using general symmetry arguments of parity and time-reversal invariance it may be shown [8] that the number of possible multipole (2^k pole) nuclear moments is severely restricted. Indeed, the only non-vanishing nuclear multipole moments are the *magnetic moments* for *odd k* and the *electric moments* for *even k*, namely the magnetic dipole ($k = 1$), electric quadrupole ($k = 2$), magnetic octupole ($k = 3$) and so on. The most important of these moments are the *magnetic dipole moment* (associated with the nuclear spin) and the *electric quadrupole moment* (caused by the departure from a spherical charge distribution in the nucleus). We shall first examine the hyperfine structure due to the magnetic dipole interaction and then discuss briefly the electric quadrupole interaction.

Magnetic dipole hyperfine structure

In 1924 W. Pauli suggested that a nucleus has a total angular momentum $\mathbf{I}$ (called 'nuclear spin') and that hyperfine structure effects might be due to magnetic interactions between the nucleus and the moving electrons of the atom, dependent upon the orientation of this nuclear spin. The eigenvalues of the operator $\mathbf{I}^2$ will be written as $I(I+1)\hbar^2$, where I is the *nuclear spin quantum number* (also often called the spin of the nucleus) or in other words the maximum possible component of $\mathbf{I}$ (measured in units of $\hbar$) in any given direction. Now the nucleus is a compound structure of nucleons (protons and neutrons) which have an intrinsic spin 1/2 and may participate in orbital motion within the nucleus. Thus the nuclear spin is compounded from the spins of the nucleons, and can also contain an orbital component. The corresponding spin quantum number I may have integer (including zero) or half-odd integer values. In the former case the nucleus is a *boson* (obeying Bose–Elnstein statistics) while in the latter case it is a *fermion* (obeying Fermi–Dirac statistics). We shall also denote by $M_I\hbar$ the eigenvalues of the operator I_z, so that the possible values of M_I are $M_I = -I, -I+1, \ldots, I$.

[8] See for example Ramsey (1953).

As we pointed out above, a nucleus may possess 2^k-pole moments, with k odd for magnetic moments and k even for electric moments. Furthermore, it may be shown [8] that a nucleus of spin quantum number I cannot have a multipole moment of order 2^n, where n is greater than $2I$. We shall begin by considering the nucleus as a point dipole with a magnetic dipole moment $\mathcal{M}_N$ proportional to the nuclear spin **I**. That is,

$$\mathcal{M}_N = g_I \mu_N \mathbf{I}/\hbar \tag{5.36}$$

where g_I is a dimensionless number (whose order of magnitude is unity) called the *nuclear g factor* or *nuclear Landé factor*. We note that g_I is positive if $\mathcal{M}_N$ lies along **I**. The quantity μ_N which appears in (5.36) is called the *nuclear magneton*; it is defined by

$$\mu_N = \frac{e\hbar}{2M_p} = \frac{m}{M_p}\mu_B \tag{5.37}$$

where m is the mass of the electron, M_p the mass of the proton and μ_B the Bohr magneton. Thus the nuclear magneton μ_N is smaller than the Bohr magneton μ_B by the factor $m/M_p = 1/1836.15$. The numerical value of the nuclear magneton is

$$\mu_N = 5.050\,78 \times 10^{-27} \text{ joule/tesla} \tag{5.38}$$

It is worth noting that (5.36) is sometimes written in units of Bohr magnetons as

$$\mathcal{M}_N = g_I' \mu_B \mathbf{I}/\hbar \tag{5.39}$$

in which case

$$g_I' = \frac{\mu_N}{\mu_B} g_I = \frac{m}{M_p} g_I = \frac{g_I}{1836.15} \tag{5.40}$$

is a very small number. Since $I\hbar$ is the maximum component of **I** in a given direction, we may also write (5.36) as

$$\mathcal{M}_N = \left(\frac{\mathcal{M}_N}{I}\right)\mathbf{I}/\hbar \tag{5.41}$$

where $\mathcal{M}_N$ is the value of the nuclear magnetic moment. In units of nuclear magnetons, we have

$$\mathcal{M}_N = g_I I \tag{5.42}$$

The values of the spin quantum number I, the nuclear Landé factor g_I and the nuclear magnetic moment $\mathcal{M}_N$ are given in Table 5.1 for the nucleons and a few nuclei.

Let us consider a hydrogenic atom with a nucleus of charge Ze such that $Z\alpha \ll 1$, and a magnetic dipole moment $\mathcal{M}_N$. We shall write the Hamiltonian of this system as

$$H = H_0 + H'_{MD} \tag{5.43}$$

where the zero-order Hamiltonian H_0 now includes the Coulomb interaction $-Ze^2/(4\pi\varepsilon_0 r)$ and the relativistic (fine structure) corrections discussed in Section 5.1 (which are of order $(Z\alpha)^2$, as seen from (5.29)) while H'_{MD} is a perturbative

Table 5.1 Values of the spin, Landé factor and magnetic moment of the nucleons and some nuclei. The notation is such that ${}^{a}_{b}X$ represents a nucleus with a total of a nucleons, b of which are protons.

Nucleus	*Spin I*	*Landé factor* g_I	*Magnetic moment* $\mathcal{M}_N$ *(in nuclear magnetons)*
proton p	1/2	5.588 3	2.792 78
neutron n	1/2	−3.826 3	−1.913 15
deuteron ${}^{2}_{1}D$	1	0.857 42	0.857 42
${}^{3}_{2}He$	1/2	−4.255	−2.127 6
${}^{4}_{2}He$	0	–	0
${}^{12}_{6}C$	0	–	0
${}^{13}_{6}C$	1/2	1.404 82	0.702 41
${}^{16}_{8}O$	0	–	0
${}^{19}_{9}F$	1/2	5.257 732	2.628 866
${}^{31}_{15}P$	1/2	2.263 20	1.131 6
${}^{39}_{19}K$	3/2	0.260 9	0.391 4
${}^{67}_{30}Zn$	5/2	0.350 28	0.875 7
${}^{85}_{37}Rb$	5/2	0.541 08	1.352 7
${}^{129}_{54}Xe$	1/2	−1.553 6	−0.776 8
${}^{133}_{55}Cs$	7/2	0.736 9	2.579
${}^{199}_{80}Hg$	1/2	1.005 4	0.502 7
${}^{201}_{80}Hg$	3/2	−0.371 13	−0.556 7

term due to the presence of the magnetic dipole moment $\mathcal{M}_N$. This term will clearly lead to even smaller corrections than those corresponding to the fine structure, since the magnetic moment of the nucleus is much smaller than that of the electron. We may therefore assume that we can deal with an isolated electronic level labelled by the total electronic angular momentum quantum number j. The zero-order wave functions (eigenfunctions of H_0) are separable in the electronic and nuclear variables and are eigenfunctions of $\mathbf{J}^2$, J_z, $\mathbf{I}^2$ and I_z (where $\mathbf{J} = \mathbf{L} + \mathbf{S}$ is the total electronic angular momentum operator). Using the Dirac notation, we shall write them as $|\gamma j m_j I M_I\rangle$, where the symbol γ represents additional quantum numbers. These zero-order wave functions are $(2j + 1)(2I + 1)$-fold degenerate in m_j and M_I. We also remark that in the Pauli approximation (see Appendix 7) – which we shall adopt here – the zero-order wave functions are also eigenfunctions of $\mathbf{L}^2$ and $\mathbf{S}^2$, and will thus be written more explicitly as $|lsjm_j IM_I\rangle$.

We now examine the perturbation H'_{MD} due to the magnetic dipole moment $\mathcal{M}_N$ of the nucleus. The magnetic field due to this dipole moment will interact with both the orbital angular momentum $\mathbf{L}$ and the spin $\mathbf{S}$ of the atomic electron. We shall denote the former interaction by H'_1 and the second by H'_2, so that

$$H'_{MD} = H'_1 + H'_2 \qquad \textbf{(5.44)}$$

The term H_1' is readily evaluated as follows. The vector potential $\mathbf{A}(\mathbf{r})$ due to a point dipole located at the origin is (Jackson, 1998)

$$\mathbf{A}(\mathbf{r}) = -\frac{\mu_0}{4\pi}\left[\mathcal{M}_N \times \nabla\left(\frac{1}{r}\right)\right]$$

$$= \frac{\mu_0}{4\pi}(\mathcal{M}_N \times \mathbf{r})\frac{1}{r^3} \tag{5.45}$$

Neglecting for a moment the spin of the electron, the interaction term due to the presence of the vector potential $\mathbf{A}(\mathbf{r})$ is (see (4.28))

$$H_1' = -\frac{i\hbar e}{m}\mathbf{A}\cdot\nabla \tag{5.46}$$

Inserting (5.45) into (5.46) one obtains (Problem 5.6)

$$H_1' = \frac{\mu_0}{4\pi}\frac{2}{\hbar}\mu_B\frac{1}{r^3}\mathbf{L}\cdot\mathcal{M}_N$$

$$= \frac{\mu_0}{4\pi}\frac{2}{\hbar^2}g_I\mu_B\mu_N\frac{1}{r^3}\mathbf{L}\cdot\mathbf{I} \tag{5.47}$$

where we have used (5.36) and we recall that $\mathbf{L} = \mathbf{r}\times\mathbf{p}$. We remark that the term H_1' may be interpreted as the interaction of the nuclear dipole moment $\mathcal{M}_N$ with the magnetic field $-[\mu_0/(4\pi)]e\mathbf{L}/(mr^3)$ created at the nucleus by the rotation of the electronic charge. We also note that H_1' has non-zero matrix elements only between states for which $l \neq 0$.

Next, we find the contribution H_2' arising from the electron spin $\mathbf{S}$. The magnetic field associated with the vector potential (5.45) is

$$\mathcal{B} = \nabla\times\mathbf{A} = -\frac{\mu_0}{4\pi}\left[\mathcal{M}_N\nabla^2\left(\frac{1}{r}\right) - \nabla(\mathcal{M}_N\cdot\nabla)\frac{1}{r}\right] \tag{5.48}$$

The spin magnetic moment of the electron is $\mathcal{M}_s = -g_s\mu_B\mathbf{S}/\hbar$ so that the corresponding interaction energy is (with $g_s = 2$)

$$H_2' = -\mathcal{M}_s\cdot\mathcal{B} = 2\mu_B\mathbf{S}\cdot\mathcal{B}/\hbar \tag{5.49}$$

or

$$H_2' = \frac{\mu_0}{4\pi}\left[\mathcal{M}_s\cdot\mathcal{M}_N\nabla^2\left(\frac{1}{r}\right) - (\mathcal{M}_s\cdot\nabla)(\mathcal{M}_N\cdot\nabla)\frac{1}{r}\right]$$

$$= -\frac{\mu_0}{4\pi}\frac{2}{\hbar^2}g_I\mu_B\mu_N\left[\mathbf{S}\cdot\mathbf{I}\,\nabla^2\left(\frac{1}{r}\right) - (\mathbf{S}\cdot\nabla)(\mathbf{I}\cdot\nabla)\frac{1}{r}\right] \tag{5.50}$$

where we have used (5.36).

It is convenient to examine the term H_2' separately for the two cases $r \neq 0$ and $r = 0$. Since the hydrogenic wave functions behave like r^l at the origin, the expression of H_2' at $r = 0$ will only be relevant for states with $l = 0$ (s states). We first note that since

$$\nabla^2\left(\frac{1}{r}\right) = -4\pi\,\delta(\mathbf{r}) \tag{5.51}$$

the first term in square brackets in (5.50) vanishes for $r \neq 0$. It can also be shown (Problem 5.7) that for $r \neq 0$

$$(\mathbf{S}\cdot\nabla)(\mathbf{I}\cdot\nabla)\frac{1}{r} = -\frac{1}{r^3}\left[\mathbf{S}\cdot\mathbf{I} - 3\frac{(\mathbf{S}\cdot\mathbf{r})(\mathbf{I}\cdot\mathbf{r})}{r^2}\right], \qquad r \neq 0 \tag{5.52}$$

Hence, using (5.50) and (5.52), we have

$$\begin{aligned} H_2' &= -\frac{\mu_0}{4\pi}\frac{2}{\hbar^2}g_l\mu_B\mu_N\frac{1}{r^3}\left[\mathbf{S}\cdot\mathbf{I} - 3\frac{(\mathbf{S}\cdot\mathbf{r})(\mathbf{I}\cdot\mathbf{r})}{r^2}\right] \\ &= \frac{\mu_0}{4\pi}\frac{1}{r^3}\left[\mathcal{M}_s\cdot\mathcal{M}_N - 3\frac{(\mathcal{M}_s\cdot\mathbf{r})(\mathcal{M}_N\cdot\mathbf{r})}{r^2}\right], \qquad r \neq 0 \end{aligned} \tag{5.53}$$

which represents the dipole–dipole interaction between the magnetic moments of the electron and the nucleus. Adding the results (5.47) and (5.53), the interaction between the nuclear magnetic dipole moment and an electron for which $l \neq 0$ is seen to be

$$H'_{MD} = \frac{\mu_0}{4\pi}\frac{2}{\hbar^2}g_l\mu_B\mu_N\frac{1}{r^3}\left[\mathbf{L}\cdot\mathbf{I} - \mathbf{S}\cdot\mathbf{I} + 3\frac{(\mathbf{S}\cdot\mathbf{r})(\mathbf{I}\cdot\mathbf{r})}{r^2}\right], \qquad r \neq 0 \tag{5.54}$$

Let us now return to the expression (5.50) of H_2' and consider the case $r = 0$, which is important for s states ($l = 0$). We have already seen that the first term in square brackets in (5.50) is proportional to $\delta(\mathbf{r})$. The second term in square brackets contains a similar term proportional to $\delta(\mathbf{r})$, as we now show. Indeed, for matrix elements involving spherically symmetric states (with $l = 0$) we remark that out of the expression (with $x_1 = x$, $x_2 = y$, $x_3 = z$)

$$(\mathbf{S}\cdot\nabla)(\mathbf{I}\cdot\nabla)\frac{1}{r} = \sum_{i=1}^{3}\sum_{j=1}^{3} S_i I_j \frac{\partial^2}{\partial x_i \partial x_j}\left(\frac{1}{r}\right) \tag{5.55}$$

all terms will vanish except those with $i = j$. Each of the matrix elements of

$$\frac{\partial^2}{\partial x_1^2}\left(\frac{1}{r}\right), \qquad \frac{\partial^2}{\partial x_2^2}\left(\frac{1}{r}\right), \qquad \frac{\partial^2}{\partial x_3^2}\left(\frac{1}{r}\right)$$

must have the same value, so that for $l = 0$

$$(\mathbf{S}\cdot\nabla)(\mathbf{I}\cdot\nabla)\frac{1}{r}=\frac{1}{3}(\mathbf{S}\cdot\mathbf{I})\nabla^2\left(\frac{1}{r}\right)=-\frac{4\pi}{3}\mathbf{S}\cdot\mathbf{I}\,\delta(\mathbf{r}) \tag{5.56}$$

From these equations and the fact that the term H_1' does not contribute for states with $l = 0$, we deduce that the interaction between the nuclear magnetic dipole moment and an s electron is given by

$$\begin{aligned}H'_{\mathrm{MD}}&=\frac{\mu_0}{4\pi}\frac{2}{\hbar^2}g_I\mu_{\mathrm{B}}\mu_{\mathrm{N}}\frac{8\pi}{3}\delta(\mathbf{r})\mathbf{S}\cdot\mathbf{I}\\&=-\frac{\mu_0}{4\pi}\frac{8\pi}{3}\mathcal{M}_s\cdot\mathcal{M}_{\mathrm{N}}\,\delta(\mathbf{r}),\qquad l=0\end{aligned} \tag{5.57}$$

This expression, which is proportional to $\delta(\mathbf{r})$, is called the *Fermi contact interaction.*

We now proceed to the calculation of the *first-order energy shifts* due to the perturbations (5.54) and (5.57). We begin by considering the case $l \neq 0$, and write (5.54) more simply as

$$H'_{\mathrm{MD}}=\frac{\mu_0}{4\pi}\frac{2}{\hbar^2}g_I\mu_{\mathrm{B}}\mu_{\mathrm{N}}\frac{1}{r^3}\mathbf{G}\cdot\mathbf{I} \tag{5.58}$$

where

$$\mathbf{G}=\mathbf{L}-\mathbf{S}+3\frac{(\mathbf{S}\cdot\mathbf{r})\mathbf{r}}{r^2} \tag{5.59}$$

We have seen above that the zero-order wave functions $|lsjm_jIM_I\rangle$ are $(2j + 1)(2I + 1)$-fold degenerate in m_j and M_I. By analogy with the spin–orbit coupling discussed in Section 5.1, the diagonalisation of the perturbation is greatly simplified by introducing the total angular momentum of the atom (nucleus + electron)

$$\mathbf{F}=\mathbf{I}+\mathbf{J} \tag{5.60}$$

We shall denote by $F(F + 1)\hbar^2$ the eigenvalues of the operator $\mathbf{F}^2$ and by $M_F\hbar$ those of F_z, with $M_F = -F, -F + 1, \ldots, +F$. From the rules concerning the addition of angular momenta, the possible values of the quantum number F are given by

$$F=|I-j|,|I-j|+1,\ldots,I+j-1,I+j \tag{5.61}$$

Since F and M_F remain good quantum numbers under the application of the perturbation H'_{MD}, it is convenient to form new zero-order functions $|lsjIFM_F\rangle$ which are linear combinations of the functions $|lsjm_jIM_I\rangle$. The energy shift due to the perturbation (5.58) is then

$$\Delta E=\frac{\mu_0}{4\pi}\frac{2}{\hbar^2}g_I\mu_{\mathrm{B}}\mu_{\mathrm{N}}\left\langle lsjIFM_F\left|\frac{1}{r^3}\mathbf{G}\cdot\mathbf{I}\right|lsjIFM_F\right\rangle,\qquad l\neq 0 \tag{5.62}$$

Using the identity (A4.58) of Appendix 4 we can replace the matrix element of $\mathbf{G}\cdot\mathbf{I}$ taken between states with equal j by that of $[j(j+1)\hbar^2]^{-1}(\mathbf{G}\cdot\mathbf{J})(\mathbf{I}\cdot\mathbf{J})$. Moreover, since

$$\mathbf{F}^2 = \mathbf{I}^2 + 2\mathbf{I}\cdot\mathbf{J} + \mathbf{J}^2 \tag{5.63}$$

so that

$$\mathbf{I}\cdot\mathbf{J} = \tfrac{1}{2}(\mathbf{F}^2 - \mathbf{I}^2 - \mathbf{J}^2) \tag{5.64}$$

we have

$$\Delta E = \frac{C}{2}[F(F+1) - I(I+1) - j(j+1)] \tag{5.65}$$

with

$$C = \frac{\mu_0}{4\pi} 2g_I\mu_B\mu_N \frac{1}{j(j+1)\hbar^2}\left\langle \frac{1}{r^3}\mathbf{G}\cdot\mathbf{J}\right\rangle, \qquad l \neq 0 \tag{5.66}$$

and we have used the simplified notation $\langle\ \rangle$ for the expectation value.

The quantity $\langle r^{-3}\mathbf{G}\cdot\mathbf{J}\rangle$ is readily obtained as follows. We first note that since $\mathbf{L}\cdot\mathbf{r} = 0$, we may write

$$\begin{aligned}\mathbf{G}\cdot\mathbf{J} &= \left(\mathbf{L} - \mathbf{S} + 3\frac{(\mathbf{S}\cdot\mathbf{r})\mathbf{r}}{r^2}\right)\cdot(\mathbf{L}+\mathbf{S}) \\ &= \mathbf{L}^2 - \mathbf{S}^2 + 3\frac{(\mathbf{S}\cdot\mathbf{r})^2}{r^2}\end{aligned} \tag{5.67}$$

It is easily shown (Problem 5.7) that

$$\mathbf{S}^2 - 3\frac{(\mathbf{S}\cdot\mathbf{r})^2}{r^2} = 0 \tag{5.68}$$

so that $\mathbf{G}\cdot\mathbf{J} = \mathbf{L}^2$ and

$$\left\langle \frac{1}{r^3}\mathbf{G}\cdot\mathbf{J}\right\rangle = l(l+1)\hbar^2\left\langle\frac{1}{r^3}\right\rangle \tag{5.69}$$

Thus we have

$$\begin{aligned}C &= \frac{\mu_0}{4\pi}2g_I\mu_B\mu_N\frac{l(l+1)}{j(j+1)}\left\langle\frac{1}{r^3}\right\rangle \\ &= \frac{\mu_0}{4\pi}2g_I\mu_B\mu_N\frac{l(l+1)}{j(j+1)}\frac{Z^3}{a_\mu^3 n^3 l(l+1/2)(l+1)}, \qquad l \neq 0\end{aligned} \tag{5.70}$$

where we have used the expectation value of r^{-3} given by (3.78), and we recall that $a_\mu = a_0(m/\mu)$, μ being the reduced mass of the electron with respect to the nucleus.

Turning now to the case of s states ($l = 0$), the first-order energy shift due to the perturbation (5.57) is

$$\Delta E = \frac{\mu_0}{4\pi}\frac{2}{\hbar^2} g_I \mu_B \mu_N \frac{8\pi}{3}\langle \delta(\mathbf{r})\, \mathbf{S}\cdot\mathbf{I}\rangle, \qquad l = 0 \tag{5.71}$$

As $\mathbf{L} = 0$, we have $\mathbf{F} = \mathbf{I} + \mathbf{S}$, from which

$$\mathbf{S}\cdot\mathbf{I} = \tfrac{1}{2}(\mathbf{F}^2 - \mathbf{I}^2 - \mathbf{S}^2) \tag{5.72}$$

and therefore

$$\Delta E = \frac{C_0}{2}[F(F+1) - I(I+1) - s(s+1)], \quad s = \frac{1}{2} \tag{5.73}$$

with

$$C_0 = \frac{\mu_0}{4\pi} 2 g_I \mu_B \mu_N \frac{8\pi}{3}\langle \delta(\mathbf{r})\rangle, \qquad l = 0 \tag{5.74}$$

Now

$$\langle \delta(\mathbf{r})\rangle = \int |\psi_{n00}(r)|^2 \delta(\mathbf{r})\, d\mathbf{r} = |\psi_{n00}(0)|^2 = \frac{Z^3}{\pi a_\mu^3 n^3} \tag{5.75}$$

where we have used the result (3.65). Thus

$$C_0 = \frac{\mu_0}{4\pi}\frac{16}{3} g_I \mu_B \mu_N \frac{Z^3}{a_\mu^3 n^3} \tag{5.76}$$

Comparing (5.65) and (5.73), and recalling that $j = s = 1/2$ for s states, we see that for both cases $l \neq 0$ and $l = 0$ we have

$$\Delta E = \frac{C}{2}[F(F+1) - I(I+1) - j(j+1)] \tag{5.77}$$

with

$$C = \frac{\mu_0}{4\pi} 4 g_I \mu_B \mu_N \frac{1}{j(j+1)(2l+1)} \frac{Z^3}{a_\mu^3 n^3} \tag{5.78}$$

Using atomic units and introducing the fine structure constant α, we may also display this result (writing explicitly the electron mass m) as

$$\Delta E = \frac{1}{2}\frac{m}{M_p} g_I \frac{Z^3\alpha^2}{n^3}\left(\frac{\mu}{m}\right)^3 \frac{F(F+1) - I(I+1) - j(j+1)}{j(j+1)(2l+1)} \text{ a.u.} \tag{5.79}$$

For a given nucleus having a spin quantum number I, a fine structure atomic energy level corresponding to fixed values of l and j is therefore split further into hyperfine components labelled by F. Since the energy correction does not depend on M_F, each of these hyperfine energy levels is $(2F + 1)$-fold degenerate. The

possible values of F being $|I-j|, |I-j|+1, \ldots, I+j$ (see (5.61)), the number of hyperfine structure components corresponding to a fine structure energy level is the smaller of the two numbers $(2j+1)$ and $(2I+1)$. These components are said to form a *hyperfine structure multiplet*. As an example, we show in Fig. 5.10 a schematic drawing of the hyperfine structure splitting of the $n=1$ and $n=2$ levels of 'ordinary' hydrogen (H) and deuterium (D). For 'ordinary' hydrogen the spin of the nucleus is just the spin of the proton, $I=1/2$, and since $j=1/2, 3/2, \ldots$ we always have hyperfine *doublets*. On the other hand, for deuterium the spin of the nucleus is $I=1$, so that we have doublets for $j=1/2$ and triplets for the other values of j.

We remark from (5.78) that since the quantity C is independent of F the *energy difference* between two neighbouring hyperfine levels – called *hyperfine separation* – is just

$$\Delta E(F) - \Delta E(F-1) = CF \tag{5.80}$$

and is thus proportional to F. This is an example of an *interval rule*. From (5.79) we also see that the energy separation δE between the two outermost components of the hyperfine multiplet (corresponding to the values $F_1 = I+j$ and $F_2 = |I-j|$ of the quantum number F) is given in atomic units by

$$\delta E = \frac{m}{M_p}\left(\frac{\mu}{m}\right)^3 g_I \frac{2Z^3\alpha^2}{n^3(j+1)(2l+1)} \times \begin{cases} I+1/2 & \text{for } j \leqslant I \\ \dfrac{I(j+1/2)}{j} & \text{for } j \geqslant I \end{cases} \tag{5.81}$$

The *hyperfine structure of spectral lines* resulting from the magnetic dipole interaction may be obtained (in a way similar to the fine structure discussed in Section 5.1) by combining the above results with the *selection rules* for electromagnetic transitions between energy levels. For *electric dipole transitions* the selection rules obtained in Section 5.1 ($\Delta l = \pm 1$ and $\Delta j = 0, \pm 1$) remain valid, and in addition it may be shown that the quantum number F obeys the selection rule

$$\Delta F = 0, \pm 1 \tag{5.82}$$

the transition $F=0 \rightarrow F=0$ being excluded. Examples of allowed hyperfine transitions are shown in Fig. 5.11. We note that transitions between levels having the same value of j but different values of F can also take place. These transitions are in the microwave region and are generally weak, so that they are best observed by using stimulated emission techniques.

The hyperfine transitions, observed by optical or microwave spectroscopy, can be used to determine the spin I and magnetic dipole moment $\mathcal{M}_N = g_I I$ of the nucleus. Indeed, the maximum hyperfine multiplicity of levels with large enough j gives $(2I+1)$ and the hyperfine separation allows the determination of the nuclear Landé factor g_I. Using the generalisation of the above equations for complex atoms (see Chapter 9), the dipole magnetic moments of many nuclei have been obtained.

The hyperfine structure of the $1s_{1/2}$ ground state of 'ordinary' hydrogen (H) is of particular interest, because in this case very elaborate calculations can be carried

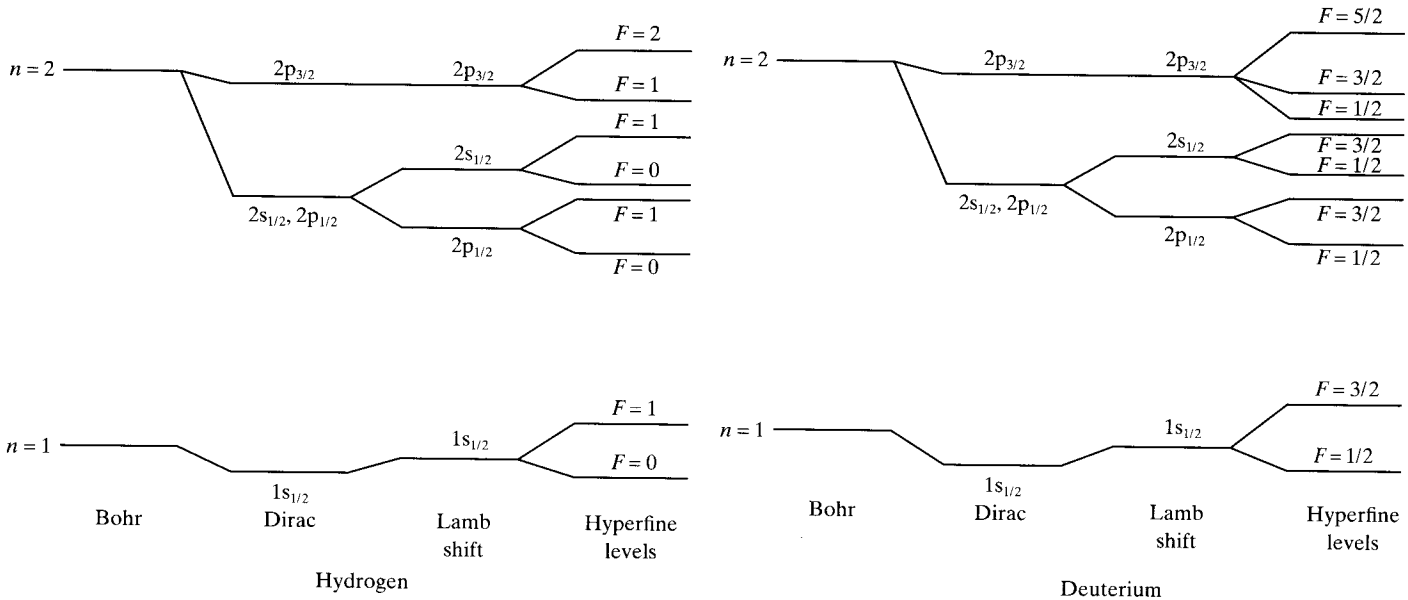

Figure 5.10 The splitting of the $n = 1$ and $n = 2$ levels of hydrogen and deuterium. The splittings are not to scale and are magnified from the left to the right of the diagram.

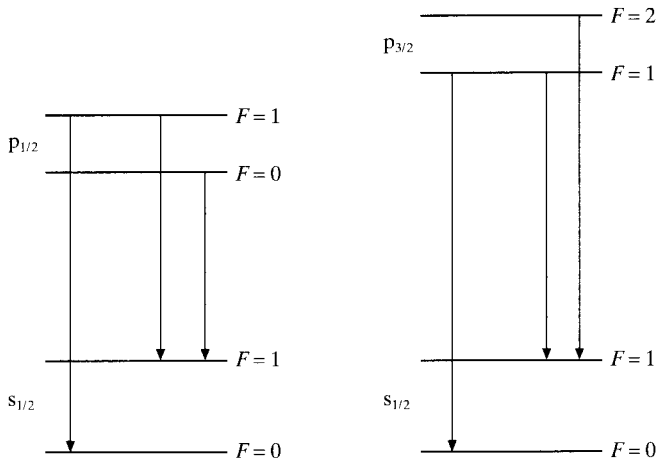

Figure 5.11 Allowed dipole transitions between n'p and ns levels of hydrogen. There is no restriction on n' and n, and the case $n' = n$ is allowed.

out and compared with extremely high-precision measurements, performed by using atomic beam magnetic resonance methods [9]. Since the proton spin is $I = 1/2$ and the level $1s_{1/2}$ has a total electronic angular momentum quantum number $j = 1/2$, this level splits into two hyperfine components corresponding to the values $F = 0$ and $F = 1$, the state with $F = 0$ being the ground state (see Fig. 5.10). Using (5.81) we see that the energy difference between the two hyperfine levels is given in atomic units by

$$\delta E = \frac{4}{3}\frac{m}{M_p}\left(\frac{\mu}{m}\right)^3 g_p \alpha^2 \tag{5.83}$$

where $g_p = 5.5883$ is the Landé factor of the proton. From this result we find that the frequency $\nu = \delta E/h$ of the transition between the two hyperfine levels (which is a magnetic dipole transition) is $\nu \simeq 1420$ MHz, the corresponding wavelength being $\lambda \simeq 21$ cm. The 'hydrogen maser', invented in 1960 by H.M. Goldenberg, D. Kleppner and N.F. Ramsey (see Section 15.1), has given very accurate data for the hyperfine frequency ν. By comparing with the frequency of a caesium atomic clock (see Section 16.5) used as a reference, the best value of ν obtained by using the hydrogen maser is

$$\nu = (1\,420\,405\,751.766\,7 \pm 0.000\,9)\ \text{Hz} \tag{5.84}$$

which is one of the most accurately measured quantities in physics.

It is gratifying to note that the simple theory presented above agrees with this result to within about 0.1 per cent. Much better agreement between theory and

[9] Magnetic resonance methods are discussed in Chapter 16. See also Ramsey (1953).

experiment can be obtained by including various corrections in the theoretical calculations. The most important of these is the introduction of the *anomalous magnetic moment of the electron*, according to which the spin gyromagnetic ratio g_s of the electron is slightly different from the value $g_s = 2$ predicted by the Dirac theory [10].

We also remark that the transition between the two hyperfine levels $F = 1$ and $F = 0$ of the ground state of hydrogen plays a very important role in *radio-astronomy*. Indeed, from the analysis of the intensity of the 21 cm radio-frequency radiation received, the astronomers have been able to learn a great deal about the distribution of neutral hydrogen atoms in interstellar space, as we shall see in Chapter 16.

Electric quadrupole hyperfine structure

A second important characteristic of the structure of a nucleus is the *electric quadrupole moment*. It is a symmetric, second-order tensor whose components Q_{ij} are defined in the following way. Let $\mathbf{R}_p$ be the coordinate of a proton with respect to the centre of mass of the nucleus, and let $X_{p1} = X_p$, $X_{p2} = Y_p$, $X_{p3} = Z_p$ be its Cartesian components. Then

$$Q_{ij} = \sum_p 3X_{pi}X_{pj} - \delta_{ij}R_p^2 \qquad (i, j = 1, 2, 3) \tag{5.85}$$

where the sum is over all the protons in the nucleus. It is customary to define the *magnitude Q of the electric quadrupole moment* as the average value of the component $Q_{zz} \equiv Q_{33}$ in the state $|I, M_I = I\rangle$. That is,

$$\begin{aligned} Q &= \langle I, M_I = I | Q_{zz} | I, M_I = I \rangle \\ &= \left\langle I, M_I = I \left| \sum_p 3Z_p^2 - R_p^2 \right| I, M_I = I \right\rangle \end{aligned} \tag{5.86}$$

The quantity Q has the dimensions of an area and is often measured in barns (10^{-24} cm^2). For example, the deuteron has an electric quadrupole moment of magnitude $Q = 0.0028$ barns. It is clear from (5.86) that a nucleus whose charge distribution is spherically symmetric has no electric quadrupole moment, since then the average value of $3Z_p^2$ is equal to that of $R_p^2 = X_p^2 + Y_p^2 + Z_p^2$. In fact the value of Q gives a measure of the deviation from a spherical charge distribution in the nucleus. If the nuclear charge distribution is elongated along the direction of $\mathbf{I}$ (prolate), then $Q > 0$; on the other hand $Q < 0$ if the charge distribution is flattened (oblate).

---

[10] The quantity $a = (g_s - 2)$ has been measured with very high accuracy by R.S. Van Dyck, Jr, P.B. Schwinberg and H.G. Dehmelt in 1987 to give the value $a = (1.159\,652\,188\,4 \pm 0.000\,000\,004\,3) \times 10^{-3}$. The current theoretical result, calculated by using quantum electrodynamics, is $(1.159\,652\,2 \pm 0.000\,000\,2) \times 10^{-3}$, the main source of inaccuracy being uncertainties of the order of 10^{-7} in the value of the fine structure constant α.

The interaction energy H'_{EQ} between the electric quadrupole moment of the nucleus and the electrostatic potential V_e created by an electron at the nucleus was first obtained by H. Casimir. Provided I and j are both good quantum numbers, it is given in atomic units by [11]

$$H'_{EQ} = B\frac{\frac{3}{2}\mathbf{I}\cdot\mathbf{J}(2\mathbf{I}\cdot\mathbf{J}+1) - \mathbf{I}^2\mathbf{J}^2}{2I(2I-1)j(2j-1)} \tag{5.87}$$

where the *quadrupole coupling constant* B is given by

$$B = Q\left\langle\frac{\partial^2 V_e}{\partial z^2}\right\rangle \tag{5.88}$$

Here

$$\left\langle\frac{\partial^2 V_e}{\partial z^2}\right\rangle = \left\langle j, m_j = j\left|\frac{\partial^2 V_e}{\partial z^2}\right| j, m_j = j\right\rangle = -\left\langle j, m_j = j\left|\frac{3z^2 - r^2}{r^5}\right| j, m_j = j\right\rangle \tag{5.89}$$

is the average gradient of the electric field produced by the electron at the nucleus.

The first-order energy shift due to the electric quadrupole interaction (5.87) is

$$\begin{aligned}\Delta E &= \langle jIFM_F|H'_{EQ}|jIFM_F\rangle \\ &= \frac{B}{4}\frac{\frac{3}{2}K(K+1) - 2I(I+1)j(j+1)}{I(2I-1)j(2j-1)}\end{aligned} \tag{5.90}$$

where

$$K = F(F+1) - I(I+1) - j(j+1) \tag{5.91}$$

Since $\langle\partial^2 V_e/\partial z^2\rangle$ vanishes when the electron charge distribution is spherically symmetric, there is no quadrupole energy shift for s states. We recall that the nuclei having no spin ($I = 0$) or a spin $I = 1/2$ have no electric quadrupole moment, so that the energy shift (5.90) also vanishes in this case.

Adding the electric quadrupole correction (5.90) to the magnetic dipole energy shift (5.77) we find that the total hyperfine structure energy correction is given by

$$\Delta E = \frac{C}{2}K + \frac{B}{4}\frac{\frac{3}{2}K(K+1) - 2I(I+1)j(j+1)}{I(2I-1)j(2j-1)} \tag{5.92}$$

Because its dependence on the quantum number F is different from that of the magnetic dipole correction (5.77), we see that the electric quadrupole correction causes a *departure from the interval rule* (5.80).

[11] See for example Casimir (1963) or Ramsey (1953).

It is worth noting that the hyperfine energy levels obtained after the correction (5.92) has been applied are still independent of the quantum number M_F, and hence are $(2F+1)$-fold degenerate. This degeneracy can be removed by applying an external magnetic field. We shall return to this *Zeeman effect in hyperfine structure* in Chapter 9.

Isotope shifts

We now consider briefly the *isotope shifts*, which do not give rise to splittings of the energy levels. As we pointed out above, these isotope shifts are caused by two effects: the *mass effect* (due to the fact that the nuclear mass is finite) and the *volume effect* (arising from the distribution of the nuclear charge within a finite volume).

For one-electron atoms the mass effect is readily taken into account by the introduction of the *reduced mass* $\mu = mM/(m+M)$, as we saw in Chapters 1 and 3. For the case of atoms with more than one electron the finiteness of the nuclear mass gives rise to an additional energy shift called the *mass polarisation correction*, which will be examined in Chapter 7.

W. Pauli and R. Peierls first pointed out in 1931 that the difference in nuclear volume between isotopes can produce an isotope shift. Indeed, since the protons in the nucleus are distributed in a finite nuclear volume, the electrostatic potential inside the nucleus deviates from the $1/r$ law, and depends on the proton distribution within the nucleus. In order to obtain an estimate of this volume effect, let us consider a simple model of the nucleus, such that the nuclear charge is distributed in a uniform way within a sphere of radius

$$R = r_0 A^{1/3} \tag{5.93}$$

where A is the mass number of the nucleus, and r_0 is a constant whose value is given approximately by $r_0 \simeq 1.2 \times 10^{-15}$ m. In this model, the electrostatic potential $V(r)$ due to the nucleus is easily shown to be (Problem 5.8)

$$V(r) = \begin{cases} \dfrac{Ze^2}{(4\pi\varepsilon_0)2R}\left(\dfrac{r^2}{R^2} - 3\right) & r \leqslant R \\ -\dfrac{Ze^2}{(4\pi\varepsilon_0)r} & r \geqslant R \end{cases} \tag{5.94}$$

To simplify the problem further, we shall assume that the unperturbed Hamilionian H_0 is the hydrogenic Hamiltonian (5.1) and that the perturbation H' is just the difference between the interaction (5.94) and the Coulomb interaction $-Ze^2/(4\pi\varepsilon_0 r)$. Thus all other effects (such as the relativistic corrections) are neglected and we have

$$H' = \begin{cases} \dfrac{Ze^2}{(4\pi\varepsilon_0)2R}\left(\dfrac{r^2}{R^2} + \dfrac{2R}{r} - 3\right) & r \leqslant R \\ 0 & r \geqslant R \end{cases} \tag{5.95}$$

The first-order energy shift due to this perturbation is

$$\Delta E = \langle \psi_{nlm} | H' | \psi_{nlm} \rangle$$
$$= \frac{Ze^2}{(4\pi\varepsilon_0)2R} \int_0^R |R_{nl}(r)|^2 \left(\frac{r^2}{R^2} + \frac{2R}{r} - 3 \right) r^2 \, dr \tag{5.96}$$

where we have used (3.53) and the fact that the spherical harmonics are normalised on the unit sphere. Inside the small region $r \leqslant R$ we may write $R_{nl}(r) \simeq R_{nl}(0)$. Moreover, since $R_{nl}(0)$ vanishes except for s states ($l = 0$), we have, after a straightforward calculation (Problem 5.9),

$$\Delta E \simeq \frac{Ze^2}{4\pi\varepsilon_0} \frac{R^2}{10} |R_{n0}(0)|^2$$
$$\simeq \frac{Ze^2}{4\pi\varepsilon_0} \frac{2\pi}{5} R^2 |\psi_{n00}(0)|^2, \qquad l = 0 \tag{5.97}$$

while $\Delta E \simeq 0$ for states with $l \neq 0$. Using (3.65) we have explicitly

$$\Delta E \simeq \frac{e^2}{4\pi\varepsilon_0} \frac{2}{5} R^2 \frac{Z^4}{a_\mu^3 n^3}, \qquad l = 0 \tag{5.98}$$

The quantity which is measured experimentally is the difference δE of energy shifts between two isotopes, whose charge distributions have radii R and $R + \delta R$, respectively. We thus find to first order in δR

$$\delta E \simeq \frac{Ze^2}{4\pi\varepsilon_0} \frac{4\pi}{5} R^2 |\psi_{n00}(0)|^2 \frac{\delta R}{R}$$
$$\simeq \frac{e^2}{4\pi\varepsilon_0} \frac{4}{5} R^2 \frac{Z^4}{a_\mu^3 n^3} \frac{\delta R}{R} \tag{5.99}$$

We note that the isotope with the larger radius has the higher energy value, and this is confirmed by experiment. We also see that δE increases when Z increases and n decreases, so that the most important volume effects occur for low-lying s states (and in particular the ground state) of hydrogenic atoms with larger Z.

So far we have only considered 'ordinary' hydrogenic atoms (ions) containing a nucleus and an electron. As we pointed out in Chapter 3, there exist also 'exotic atoms' such as muonic atoms, in which a muon μ^- forms a bound system with a nucleus. We also noticed in Chapter 3 that since the mass of the muon μ^- is about 207 times larger than the electron mass, the Bohr radius associated with muonic atoms is much smaller than for 'ordinary' (electronic) atoms (see Table 3.2). We therefore expect that *hyperfine effects will be much larger for muonic atoms than for the corresponding ordinary atoms*. In particular, using the fact that the quantity a_μ is roughly 200 times smaller for a muonic atom than for an ordinary atom, we deduce from the foregoing discussion that the volume effect will be considerably magnified for muonic atoms, as we pointed out in Section 3.6.

Problems

5.1 Starting from (5.14), obtain the result (5.15) for the energy shift ΔE_1.

5.2 Using (5.24) and (5.25), obtain the expressions (5.26) for the energy shift ΔE_2.

5.3 Obtain the total relativistic energy shift (5.28) by using (5.15), (5.26) and (5.27).

5.4 Show that the expression (5.29) agrees up to order $(Z\alpha)^2$ with the formula (5.30) obtained by solving the Dirac equation.

5.5 Show that the ratio of the probabilities of the transitions in atomic hydrogen $np_{3/2} \rightarrow n's_{1/2}$ and $np_{1/2} \rightarrow n's_{1/2}$ is 2:1.

5.6 Verify that the expression (5.47) follows from (5.45) and (5.46).

5.7 Prove the relations (5.52) and (5.68).

5.8 Consider an electron in the electrostatic field of a nucleus of charge Ze, and of mass number A. If the nuclear charge is distributed uniformly within a sphere of radius $R = r_0 A^{1/3}$ where $r_0 \simeq 1.2 \times 10^{-15}$ m,

(a) show that the potential is given by (5.94);
(b) verify that the first-order energy shift due to the perturbation (5.95) is given by (5.97).